PCCP

PAPER

View Article Online
View Journal | View Issue

Cite this: *Phys. Chem. Chem. Phys.*, 2019, **21**, 6042

Solvent organization around the noncanonical part of tyrosine modulates its fluorescence properties†

Tonima Nandy, Saptarsi Mondal and Prashant Chandra Singh *

Received 15th October 2018,
Accepted 15th February 2019

DOI: 10.1039/c8cp06410e

rsc.li/pccp

Noncanonical amino acids are important molecules that enhance the functionality of proteins, and they are also intensively used in therapeutics. In this paper, we have investigated the fluorescence properties of the noncanonical amino acid 2-(trifluoromethyl) tyrosine (TFTyr) in three different alcohols, namely ethanol (ETH), monofluoroethanol (MFE), and trifluoroethanol (TFE), using spectroscopy, quantum chemical calculations and MD simulations. Further, we have compared its fluorescence properties with those of its canonical derivative tyrosine (Tyr) in the same solvents to understand the role of the noncanonical $-CF_3$ group in the fluorescence properties of TFTyr. The excited state lifetime of Tyr decreases monotonically with the fluorination of ETH, whereas the trend is opposite in the case of TFTyr. The calculated emission maxima of different-sized clusters of TFTyr and TFE, as well as comparison with the experimental values, suggest that the role of F···F, O–H···O and N–H···O interactions is significant. Quantum chemical calculations as well as MD simulations suggest that alcohols have a preferred orientation around the noncanonical $-CF_3$ group of TFTyr and the fluorescence properties of TFTyr are very sensitive to the mode of interaction of the $-CF_3$ group of TFTyr with alcohols. This study suggests that TFTyr can be a potential candidate for exploring the role of solvent environments in several biological processes.

Introduction

The genetic code of the universal biosphere contains twenty amino acids for biosynthesis of proteins and controls the various functionalities of each organism. However, it has been found that several higher levels of complexity are needed for the functionalities of proteins, which are achieved by post-translational modification as well as the use of several cofactors for enzymes.[1–3] The functional limitation of proteins due to the limited number of canonical amino acids has led to research in the field of protein engineering where several noncanonical amino acids can be incorporated into proteins by site or residue mutagenesis, which enhances the functionalities as well as providing possibilities for the novel chemistry of proteins.[4–11] The application of noncanonical amino acids is not only limited to the modification of the functionality and properties of proteins, but their use in therapeutics.[12–14]

Fluorinated amino acids are an important class of noncanonical amino acids which have been intensively used for the modifications of proteins' functionality, lipid membrane, protein–protein interactions and enhancement of catabolic activity.[15–20] Several approaches have been adopted for the insertion of fluorinated amino acids into peptides and proteins with minimal effects on their structure and biological activity.[21–23] Indeed, it has been found that the insertion of fluorinated amino acids increases the stability of various kinds of proteins against denaturing agents as compared to non-fluorinated amino acids.[21,22] The substitution of fluorocarbon (C–F) in place of hydrocarbon (C–H) induces unique but important physicochemical properties. Fluorocarbon and hydrocarbon both possess hydrophobic natures; however, the properties of fluorocarbon groups are distinctly different.[24,25] The dipole moment of C–F is higher and its direction is opposite to the C–H group. The higher dipole of C–F generates strong electrostatic interactions with polar groups, due to which the hydrophobicity of fluorocarbons is described as polar hydrophobicity.[26] The C–F bond length is longer than C–H, which increases the volume of fluorine-containing molecules. Moreover, due to the high electronegativity and small size, the polarizability of fluorocarbons is less than hydrocarbons. Due to these unique properties, molecules

Department of Spectroscopy, Indian Association for the Cultivation of Science, Kolkata, 700032, India. E-mail: sppcs@iacs.res.in

† Electronic supplementary information (ESI) available: A table showing the maxima of emission of TFTyr in ETH and TFE using different methods and solvent models, the radial distribution of solvents near the different binding sites of amino acids both in their zwitterionic and neutral states and in ground as well as excited states, a pictorial representation of solvent molecules around the neutral form of TFTyr, optimized structures of TFTyr-TFE complexes showing their respective emission values, ONIOM results, AIM images of different clusters of TFTyr in TFE and the method of calculation of the quantum yield. See DOI: 10.1039/c8cp06410e

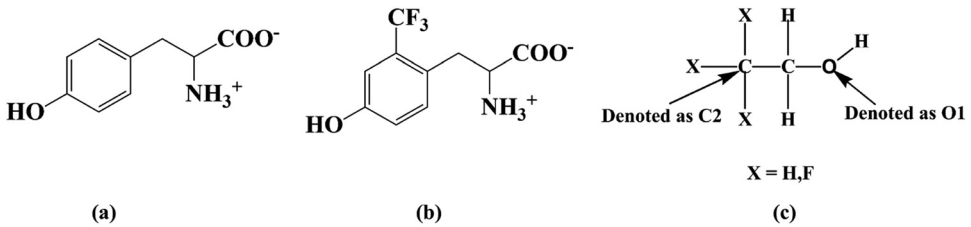

Fig. 1 The zwitterionic structures of (a) Tyr and (b) TFTyr and (c) the abbreviations of different parts of the alcohols used in MD simulations.

containing fluorocarbon groups prefer to self-aggregate through fluorous (F···F) interactions.[27,28]

The unique properties of fluorocarbon groups tend to affect the hydration as well as hydrogen bonding phenomena of fluorocarbon-containing peptides and proteins. Zewail and coworkers have shown that the side chain fluorination of proteins exerts strong electrostatic drag on water molecules, which slows down reorientation of water near the fluorinated surface.[29] Kunston and coworkers have incorporated 5-fluorotryptophan in monellin and found that the incorporation of fluorinated tryptophan suppresses electron transfer quenching, thereby masking the pseudo-time-dependent fluorescence Stokes shift, which in turn helps to provide a distinct ultrafast relaxation resulting from the increased solvent and protein response.[30] Krishnamoorthy and coworkers have demonstrated that the substitution of 5-fluorotryptophan decreases the lifetime heterogeneity of proteins as compared to tryptophan.[31] These studies have established that the fluorination of amino acids changes their properties drastically; however, the molecular level understanding about the role of noncanonical moieties in the solvent organization, and the nature of different interactions with solvent molecules imparting different properties, have not been investigated extensively.

In this paper, we have investigated the fluorescence properties of the noncanonical amino acid 2-(trifluoromethyl) tyrosine (TFTyr) in three different solvents, namely, ethanol (ETH), monofluoroethanol (MFE) and trifluoroethanol (TFE), using spectroscopy, quantum chemical calculations and molecular dynamics (MD) simulations (the zwitterionic structures are shown in Fig. 1). We have chosen TFTyr as it has been suggested that trifluoromethyl and fluorinated derivatives of tyrosine can be used as inhibitors for tyrosine hydroxylase as well as therapeutics.[12–14,32] Further, we have compared the behavior of TFTyr in alcoholic solvents with that of tyrosine (Tyr) in order to understand the role of the noncanonical $-CF_3$ moiety in its fluorescence properties. Fluorinated ethanol derivatives (fluoro-ETHs) have been chosen as it is well known that they stabilize the secondary structure of proteins as well as inducing changes in their conformation. Moreover, fluoro-ETHs can undergo fluorous interactions among themselves[33,34] as well as with the noncanonical amino acid TFTyr, which may result in different photophysical properties from those of Tyr.

Methods

(a) Experimental setup and materials

A HORIBA Jobin Yvon Fluorolog 3 spectrometer was used to measure the steady state emission spectra of the probe in different solvents. Fluorescence intensity decays were measured using the time-correlated single-photon counting (TCSPC) setup of an IBH fluorocube. A picosecond diode laser of 280 nm (IBH nanoleds) was used as an excitation source. The emission was collected under magic angle polarization and detected using a multiple channel photomultiplier (MCP, Hamamatsu, 5000U-09). The typical full width at half maximum of the system was measured to be ~700 ps using a liquid scatterer. Fluorescence intensity decays were analyzed using IBH DAS6 software and were deconvoluted with the instrument response profile. The reduced chi-square (χ^2) value as well as the distribution of the weighted residuals has been used to check the reliability of the data. The obtained values of χ^2 were close to one and the weighted residuals were randomly distributed around zero, indicating a high goodness of fit. The quantum yield of all the systems has been calculated using the standard method and details of the method have been provided in the ESI.†

ETH (99.9%), MFE (98%) and TFE (99.5%) were purchased from Spectrochem (Mumbai, India) and distilled as well as purged with N_2 before and during the measurements to make sure that there was no water content in the solution. Tyr and TFTyr were purchased from Spectrochem (99%) and Netchem USA (99%), respectively. The probe concentration used in this study is ~10 μM. All measurements were carried out at ambient temperature (~25 °C).

(b) Molecular dynamics simulations

The MD simulations have been carried out using the all atom simulation method incorporated in the GROMACS molecular dynamics simulation package (version 5.1).[35] For ETH and MFE, all atom Amber99sb-ildn force field parameters available in the GROMACS topology were used.[35,36] For TFE, we have used the Amber99sb-ildn force field parameters proposed by Fironi *et al.* and modified by Gerig *et al.* to include the non-bonding effects of fluorine.[37,38] The all atom force field parameters for Tyr and TFTyr have been generated using the ATB server[27,28,39] where partial charges have been recalibrated using the RESP-A1 model for maximum accuracy and reproducibility.[40] In order to match the experimental concentration of the probe (in μM concentration range), one has to take 10^6 solvent molecules per probe molecule. However, for efficient simulation, we have taken one amino acid and solvated it in ~4000 alcohol molecules to generate a bulk like environment. For each case, we have run 1000 steps of steepest descent followed by 10 000 steps of the conjugate gradient energy minimization algorithm to exclude all unfavorable interactions from the initial configuration.

Further, each trajectory was equilibrated in the *NPT* ensemble at 300 K temperature and 1 bar pressure for 1 ns. Subsequently, the equilibrated configuration was subjected to a production run of another 50 ns in the *NPT* ensemble at 300 K and 1 bar pressure. The temperature and pressure were kept constant using the Berendsen thermostat[41] with a time constant (τ) of 0.1 ps and the Parrinello–Rahman barostat[42] with a τ of 1.0 ps, respectively. Electrostatic interactions were incorporated by particle mesh Ewald (PME)[43] with a grid spacing of 0.16 nm. Each simulation used a time-step of 1 fs with periodic boundary conditions. Neighbor list generation has been performed with the help of non-bonded force calculation with a grid and updated every 5 steps throughout the simulation. The MD simulation has been performed by considering the excited state charge distribution of Tyr and TFTyr in order to understand the solvent organization in the excited state of the probe molecules. The excited state charge distribution has been obtained by quantum chemical calculations. We have calculated the radial distribution $g(r)$ in the ground state as well as excited state near to the different binding sites of the amino acids to acquire information of the solvent organization around the probe.

(c) Quantum chemical calculations

Different conformers of the zwitterionic form of Tyr and TFTyr were generated using the MacroModel package.[44] The ten lowest energy conformers of Tyr and TFTyr were optimized in ETH and TFE using the CAM-B3LYP/6-31+G(d,p) level of theory[45–47] to obtain their minimum energy structure. The zwitterionic form has been chosen for the quantum chemical calculations as it has been found to be significantly more populated as compared to the neutral form in the respective solvent media based on free energy calculations.[48,49] The minimum energy structures of Tyr and TFTyr in ETH and TFE were also confirmed by the angular distribution analysis of different structures obtained from the MD simulations. Both procedures provide the same minimum energy conformers of Tyr and TFTyr as shown in the ESI† (Fig. S1). The emission maxima of the most stable conformer of Tyr and TFTyr in ETH and TFE were calculated using three different solvent models, namely, the universal solvent model (SMD),[50] polarizable continuum model (PCM)[51] and integral equation formalism of PCM (IEF-PCM, using default atomic radii).[52] It has been found that the emission maxima calculated by IEF-PCM were closest to the experimental data, hence, this model has been used for all further calculations (Table S1, ESI†).

Further, different types of clusters of TFTyr with ETH and TFE have been investigated to understand the role of the $-CF_3$ group in its emission properties. First, we have performed the MD simulation of TFTyr with ETH and TFE to obtain the initial structure of the different clusters. From the MD simulations of these molecules, we have selected several structures of the solvent molecules within 8 Å of the probe and optimized them using the CAM-B3LYP/6-31+G(d,p) level of theory[45–47] to acquire the minimum energy structures. The frequency calculation of each structure in the two solvents has been performed, which only gave positive values, confirming the stable nature of the structures on the potential energy surface. Further, we have calculated the peak maxima of the emission spectra of TFTyr in ETH and TFE in order to compare with the experimental values. All the calculations have been performed using the Gaussian 09 suite of programs.[53]

Results and discussion

The steady state emission spectra of Tyr and TFTyr in ETH, MFE and TFE are shown in Fig. 2 and the peak maxima (λ_{max}) of the emission spectra for each case have been provided in Table 1. The steady state emission spectra of Tyr in ETH and MFE are structureless and the λ_{max} of the emission spectrum for MFE is slightly red shifted as compared to ETH. In contrast to ETH and MFE, the emission spectrum of Tyr in TFE is slightly structured as well as blue shifted as compared to ETH. Due to the presence of the $-CF_3$ group, the λ_{max} of the emission spectra of TFTyr in all the solvents are red shifted as compared to Tyr. In general, the trend of the shift of λ_{max} values of TFTyr in all the solvents is similar to the case of Tyr. However, the spectral features of TFTyr in TFE are different as compared to the case of Tyr. Unlike for Tyr, the emission spectrum of TFTyr in TFE is structureless, indicating that the local environment of TFTyr in TFE is essentially different from that of Tyr, and this difference is probably caused by the $-CF_3$ group of TFTyr.

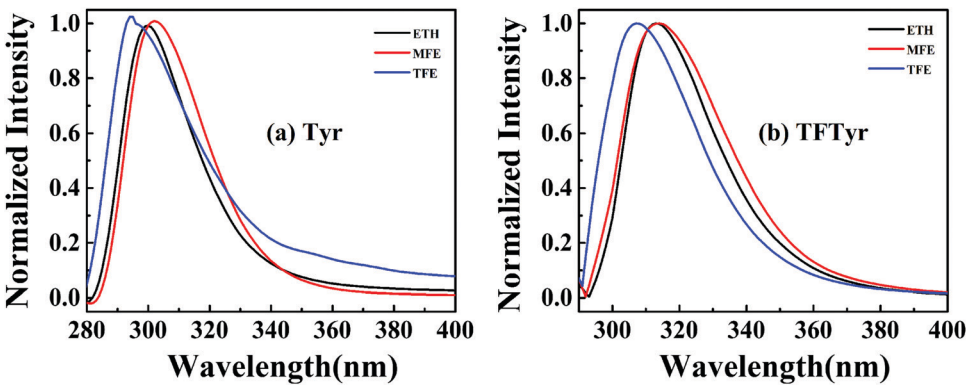

Fig. 2 The steady state emission spectra of Tyr and TFTyr in ETH (black), MFE (red) and TFE (blue), respectively.

Table 1 The peak position of steady state emission spectrum (nm), lifetime (ns), quantum yield (Φ_f), radiative rate constant (k_r) and nonradiative rate constant (k_{nr}) in s^{-1} for Tyr and TFTyr in ETH, MFE and TFE solvents. The number in parentheses next to each lifetime shows the amplitude of its components

System	Emission (nm)	Lifetime[a] (ns)	Average lifetime (ns)	Φ_f	$k_r \times 10^8$ (s^{-1})	$k_{nr} \times 10^8$ (s^{-1})
Tyr						
ETH	300	3.86 (*1.00*)	3.86	0.19	0.49	2.1
MFE	302	0.91 (*0.62*) 1.74 (*0.33*) 4.67 (*0.05*)	1.37	0.04	0.30	7.0
TFE	296	0.70 (*0.99*) 3.74 (*0.01*)	0.73	0.03	0.41	13.2
TFTyr						
ETH	312	2.18 (*1.00*)	2.18	0.10	0.43	4.16
MFE	313	2.20 (*0.98*) 7.0 (*0.02*)	2.29	0.05	0.21	4.10
TFE	308	2.46 (*1.00*)	2.46	0.10	0.36	3.70

[a] ±0.05 ns is the maximum uncertainty associated with the evaluation of lifetime value. Uncertainty has been calculated by four repeat measurements of each compound in solution.

It is well known that a steady state study provides the average properties of a molecule in a given medium. Hence, we have measured the excited state lifetime (τ) of Tyr and TFTyr in ETH and fluorinated-ETHs to explore the local environments of TFTyr as well as the effect of $-CF_3$ on their fluorescence properties. The time trace of Tyr in ETH can be fit with a single exponential, whereas it shows multi-exponential (one short and two long components) features in MFE, and bi-exponential (one short and one long) features for TFE. It is noticeable that the amplitude of the short lifetime component of Tyr in fluorinated alcohols increases while the amplitude of the long lifetime component decreases. The presence of different components of lifetime for Tyr in fluorinated alcohols probably indicates the heterogeneity of interaction between the solvents and Tyr. The long lifetime component of Tyr with significantly less amplitude in fluorinated alcohols is probably due to the interaction of the terminal fluorine of fluorinated alcohols with Tyr. The average τ value of Tyr decreases monotonically with the fluorination of ETH, which is in line with the polarity of the solvents, as the fluorination of ETH increases the polarity of the medium monotonically. The lifetime data of Tyr in alcoholic solvents suggests that the polarity of the media controls their photophysical behaviour irrespective of the possibility of a different interaction of Tyr with fluorinated ETHs than with ETH (Fig. 3).

The excited state lifetime trace of TFTyr is single exponential in ETH; however, the τ value of TFTyr is less than for Tyr. The τ value of TFTyr in fluorinated-ETHs is completely different from Tyr in the same solvents. Unlike Tyr, TFTyr in fluorinated-ETHs does not show any short lifetime components. The time trace of TFTyr in TFE depicts a single exponential feature whereas in the case of MFE, a bi-exponential feature (2.2 and 7.0 ns) has been found, in which the contribution of the 2.2 ns component is significantly larger (~98%) than the other component. Compared to the case of Tyr, the trend of τ_{av} of TFTyr in alcoholic solvents is reversed and its value is maximum for TFE followed by MFE. In ETH, the τ_{av} value of TFTyr is less than that of Tyr whereas the τ_{av} value of TFTyr is higher than that of Tyr in fluorinated alcohols.

The lifetime of any probe in any solvent medium depends upon the dipole moment of the probe, polarity of the medium and the solute–solvent interactions. The polarity of any given fluorinated solvent is constant for both the probes. The CF_3 substituent will increase the excited state dipole moment of TFTyr, which should decrease the excited state lifetime of TFTyr as compared to Tyr.[54] Indeed, the decreased τ_{av} value of TFTyr in ETH as compared to Tyr is due to the higher excited state dipole moment of TFTyr. However, the longer lifetime of TFTyr than Tyr in fluorinated alcohols indicates that the polarity of the solvent and the dipole moment of the probe are not decisive factors. Hence, it is plausible that the $-CF_3$ substituent reorganizes the solvent, making it likely that the solute–solvent interactions at the $-CF_3$ site of TFTyr with each of the fluorinated-ETHs are different, which controls the fluorescence properties of TFTyr in these solvents.

$$\Phi_F = \frac{K_r}{K_r + K_{nr}}. \quad (1)$$

$$\tau = \frac{1}{K_r + K_{nr}}. \quad (2)$$

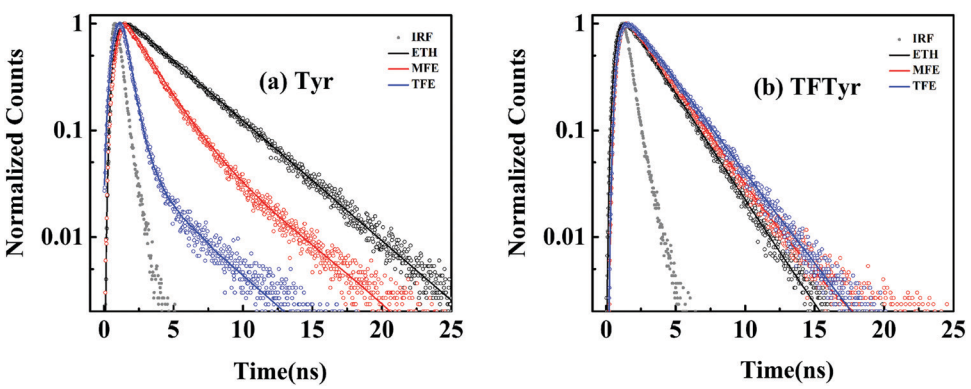

Fig. 3 The lifetime traces of Tyr (a) and TFTyr (b) in ETH (black), MFE (red) and TFE (blue), respectively. The gray dotted line depicts the instrument response function profile.

Further, we have calculated the quantum yield (ϕ), radiative (k_r) and nonradiative rate constant (k_{nr}) of Tyr and TFTyr in alcoholic solvents in order to enhance our understanding of the effect of CF_3 substitution on the photophysical properties of Tyr (the values are provided in Table 1). The ϕ values of Tyr and TFTyr in different solvents have been calculated by the standard method whereas the rate constants k_r and k_{nr} of these processes have been calculated using eqn (1) and (2). It can be seen that the change of k_{nr} is more prominent than k_r for Tyr in alcoholic solvents. The k_{nr} of Tyr in fluorinated ETHs increases successively with the increase of fluorine atoms in the solvent and its value in TFE is $\sim$6 times higher than in ETH. The trends of the change in k_r and k_{nr} suggest that the role of k_{nr} is significant for controlling the fluorescence properties of Tyr. The value of k_{nr} of TFTyr in fluorinated-ETHs is significantly decreased compared to the case of Tyr, which also suggests that $-CF_3$ substitution either indirectly changes the solvent (fluorinated-ETHs) organization around the different interacting sites of the amino acid, or fluorinated solvents may have specific interactions with the CF_3 terminus of TFTyr by changing their orientation.

The fluorescence lifetime of a molecule depends on the surrounding equilibrium solvent organization, which in turn depends on the local dielectric constant and the specific interaction between the solute and solvent molecules. Experimental studies suggest that the role of solute–solvent interaction can be important for the fluorescence properties of TFTyr. Hence, to investigate the role of solute–solvent interaction between this probe and different solvents, we have calculated the radial distribution function $g(r)$ for the different interaction sites of the probe with each solvent. For calculating $g(r)$, the chosen binding sites for the solvents were the phenolic OH group, COO^- group, and NH_3^+ group of the amino acids. These $g(r)$ values help us to understand the direct or indirect effect of the $-CF_3$ substitution on the solvent organization (results are shown in Fig. S2 and S3, ESI†). The phenolic OH group of amino acids can be either a hydrogen bond donor or an acceptor with alcoholic solvents. The $g(r)$ data for the phenolic OH group of the studied amino acids and alcohols suggests that the phenolic OH group of these amino acids acts predominantly as a donor and forms OH(amino acids)$\cdots$O(alcohols) type hydrogen bonds with the solvents (Fig. S2, ESI†). The probability of formation of OH(amino acids)$\cdots$O(alcohols) hydrogen bonds at the phenolic OH site has the same trend for Tyr and TFTyr and is largest for ETH. The decrease in the probability of OH(amino acids)$\cdots$O(alcohols) hydrogen bonding with fluoro-ETHs may be due to the increased acidity of fluorinated solvents, which makes fluorinated alcohols slightly better donors than acceptors. The higher accepting capability of the fluorinated alcohols than ETH is also supported by the fact that the $g(r)$ of O(amino acids)$\cdots$HO(alcohols) interaction increases for the fluorinated alcohols. It is also noticeable that the probability of the formation of OH(amino acids)$\cdots$O(alcohols) hydrogen bonds for TFTyr with any particular alcohol is slightly higher than for Tyr, which is probably due to the increased donor capability of the phenolic OH due to the CF_3 substitution. The trend of the $g(r)$ data for the other binding sites, namely COO^- and N–H, of Tyr and TFTyr is nearly the same in all the solvents, suggesting that the indirect effect of the CF_3 substitution on the solvent orientation around those binding sites of amino acids is not significant (Fig. S3, ESI†).

The solvent orientation around the different possible binding sites is nearly the same for both amino acids. Hence, we have investigated the solvent orientation near to the CF_3 group of TFTyr to understand their different fluorescence behaviour in these solvents. The $g(r)$ between the fluorines of CF_3 of TFTyr and the terminal carbon (C2) as well as the oxygen (O1) of the alcohols has been calculated to quantify the interaction of the solvents with the CF_3 group of TFTyr. Fig. 4 shows the $g(r)$ for the O1 (red line) and C2 (black line) of TFE with the fluorines of the CF_3 moiety of TFTyr, which depicts the clear signature of preferential solvation of the C2 terminus of TFE around the CF_3 moiety of TFTyr. We have also calculated the same $g(r)$ for ETH and MFE, which also depict the same preferential solvation of the C2 terminus of these alcohols around the CF_3 moiety of TFTyr (Fig. S4, ESI†). The orientation of the different solvents around the CF_3 moiety of TFTyr has been shown in pictorial representation (Fig. 4b–d) and clearly suggests that the CH_3 group of ETH, CH_2F group of MFE and CF_3 group of TFE are closely organized near the CF_3 moiety of TFTyr. It is important to mention that the solvent orientations around the CF_3 moiety

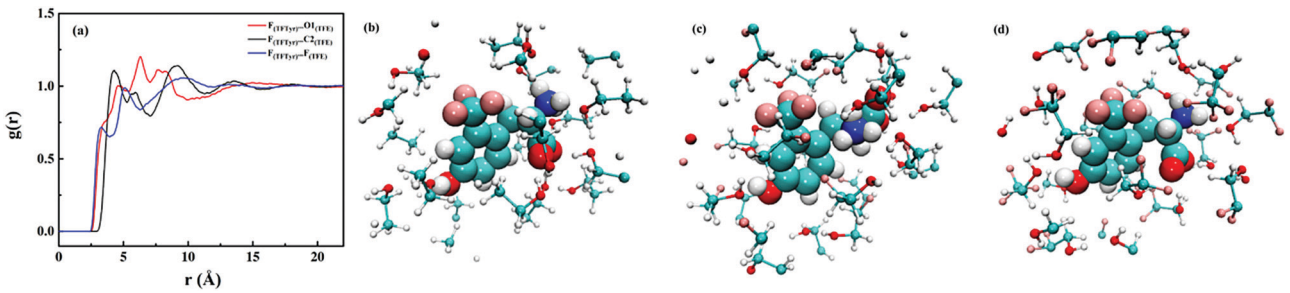

Fig. 4 Solvent organization around CF_3 moiety of TFTyr. (a) $g(r)$ of O1 (red) and C2 (black) atoms of TFE with the CF_3 moiety of TFTyr. The higher first peak value for the C2 atom suggests the preferential solvation by the C2 end of TFE. Similar preferential solvation by other alcohols is also observed (ESI,† Fig. S4). Pictorial representation of the first solvation layer around CF_3 moiety of TFTyr in (b) ETH, (c) MFE, and (d) TFE suggesting the preferential solvation by the C2 end of alcohols in all cases. Blue line in the $g(r)$ plot shows the possibility of fluorous (F$\cdots$F) interaction between the CF_3 moiety of TFTyr and the TFE solvent.

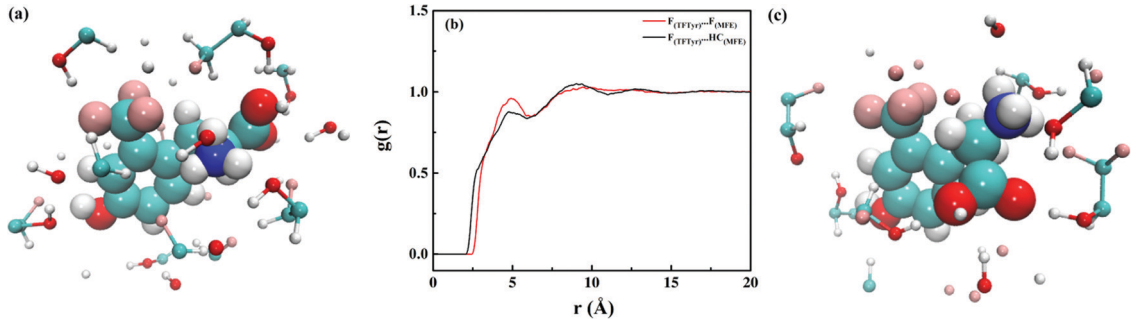

Fig. 5 Pictorial representations of the atoms present within 3.5 Å from the CF_3 moiety of TFTyr in MFE. (a) and (b) represent the $g(r)$ of F and H (C2) atoms of MFE from CF_3 moiety of TFTyr. Shifting of the first peak towards lower distances for H (C2) atom compared to F atom indicates the possibility of the formation of specific FCH(MFE)$\cdots F_3C$(TFTyr) interactions. The pictorial representations of the atoms present within 3.5 Å from the CF_3 moiety of TFTyr in TFE are shown in (c) which confirms the presence of (F$\cdots$F) interaction between the CF_3 moieties of TFTyr and TFE solvent.

of TFTyr are different from those around the other binding sites of the amino acid. At the other binding sites, the O–H(solvent)$\cdots$O(solvent) hydrogen bond between the alcohols is reorganized and the O1 terminus of the alcohols interacts with the amino acids. However, at the CF_3 moiety of TFTyr, the solvent molecules try to preserve the bulk O–H(solvent)$\cdots$O(solvent) hydrogen bond by maximizing their preferential interaction with the CF_3 moiety of TFTyr *via* the C2 terminus.

Further, we display the solvent atoms present within 3.5 Å of a fluorine atom of the CF_3 moiety of TFTyr (Fig. 5) in order to understand the interaction between the C2 terminus of alcohols and the CF_3 moiety of TFTyr. The hydrogen atom attached to the C2 group of ETH comes closer to the CF_3 moiety of TFTyr. However, in the case of MFE, the situation is slightly different as the C2 group of MFE has a CH as well as a CF group and both can compete near the CF_3 moiety of TFTyr. It can be seen that the number of hydrogen atoms of MFE molecules ($\sim$9) is more than that of fluorine atoms ($\sim$2) near to the CF_3 moiety of TFTyr, which suggests the possibility of interaction between the CH group of MFE and the CF_3 moiety of TFTyr. In order to confirm the orientation of MFE, we have calculated the $g(r)$ between the fluorines of the CF_3 moiety of TFTyr and the hydrogen (black line, Fig. 5b) as well as fluorine (red line, Fig. 5b) atoms of MFE attached to its C2 terminus. The first peak of the $g(r)$ plot between fluorines of the CF_3 moiety of TFTyr and hydrogens of MFE is more shifted than that with the fluorines of MFE (Fig. 5b), which confirms that the CH group of MFE prefers to interact with the CF_3 moiety of TFTyr through FCH(MFE)$\cdots F_3C$(TFTyr) interaction rather than HCF(MFE)$\cdots F_3C$(TFTyr) interaction. The electron withdrawing capability of fluorine makes the C–H group of MFE a stronger hydrogen bond donor, hence, the nature of the FCH(MFE)$\cdots F_3C$(TFTyr) interaction will be electrostatic whereas earlier studies have shown that the F$\cdots$F interaction is mainly dispersive in nature.[28] In the case of MFE, the electrostatic nature of the FCH(MFE)$\cdots F_3C$(TFTyr) interaction dominates over the dispersion force generated by the HCF(MFE)$\cdots F_3C$(TFTyr) interaction as the hydrogen atoms of MFE are nearer to the CF_3 moiety of TFTyr than the fluorines of MFE are. Interestingly, in the case of TFE, fluorine attached to the terminal C2 of TFE comes close to the fluorine of the CF_3 moiety of TFTyr, which creates a fluorous (F$\cdots$F) interaction between the CF_3 moiety of TFTyr and the TFE solvent (Fig. 5c). The presence of a fluorous interaction is also confirmed by the calculation of $g(r)$ between the fluorine(s) of TFE and TFTyr as shown in the blue line of Fig. 4a. In TFE, the dispersive fluorous interaction between the CF_3 moiety of TFTyr and CF_3 group of TFE dominates in contrast to the case of MFE, where the electrostatic interaction prevails. We have also performed MD simulations of the neutral Tyr and TFTyr in different solvents and the trends of the results are similar to those of the zwitterionic state (Fig. S5–S7, ESI†).

Further, we have calculated the $g(r)$ for the different interactions of ETH and TFE with TFTyr using their excited state charge distribution and compared them with the ground state case as shown in Fig. S8 (ESI†). It can be seen that qualitatively the trend of the $g(r)$ is the same in the excited state as well as the ground state except that the $g(r)$ for F$\cdots$F interaction becomes more prominent in the excited state. The trend of the $g(r)$ data suggests that solvent organization does not change significantly in the excited state as compared to the ground

Table 2 The emission maxima (nm) of the Tyr and TFTyr monomers along with the 1 : 3 clusters of TFTyr in ETH and TFE calculated using the CAM-B3LYP/6-31+g(d,p) level of theory. The polarizable continuum model using the integral equation formalism (IEF-PCM) variant has been used to incorporate the effect of the respective solvents

System	Solvent	Calculated (λ_{max})	Experimental (λ_{max})
Monomer			
Tyr	ETH	267	300
	TFE	264	296
TFTyr	ETH	310	312
	TFE	308	308
1 : 3 cluster of TFTyr			
a	ETH	313	312
b		288	
c		304	
d	TFE	303	308
e		289	
f		302	
g		306	
h		295	
i		287	
j		286	

state of the probe molecule although the fluorine group of the probe molecule approaches closer to the fluorine of TFE, causing the slightly stronger F···F interaction in the excited state as compared to the ground state.

Finally, we have calculated the emission maxima of Tyr and TFTyr in both ETH and TFE using the quantum chemical CAM-B3LYP/6-31+G(d,p) level of theory[45–47] and the results are provided in Table 2. In general, the absolute values of the calculated emission maxima of the fluorescence spectra of TFTyr in ETH and TFE are in good agreement with the experimental values; however, the calculated emission maximum is underestimated for Tyr. Nevertheless, the trend of the change of the calculated values of the emission maxima of Tyr and TFTyr in ETH and TFE is similar to the experimental trend. For example, upon the substitution of CF_3 into Tyr, the calculated value of the emission maximum is red shifted in accord with the experimental value. Similarly, the calculated emission maxima of Tyr and TFTyr are blue shifted in TFE as compared to ETH, in agreement with the experimental values.

To probe the different fluorescence behaviour of TFTyr in TFE, we have calculated the emission maxima of different sizes of clusters (1:1, 1:2 and 1:3) of TFTyr and TFE at three

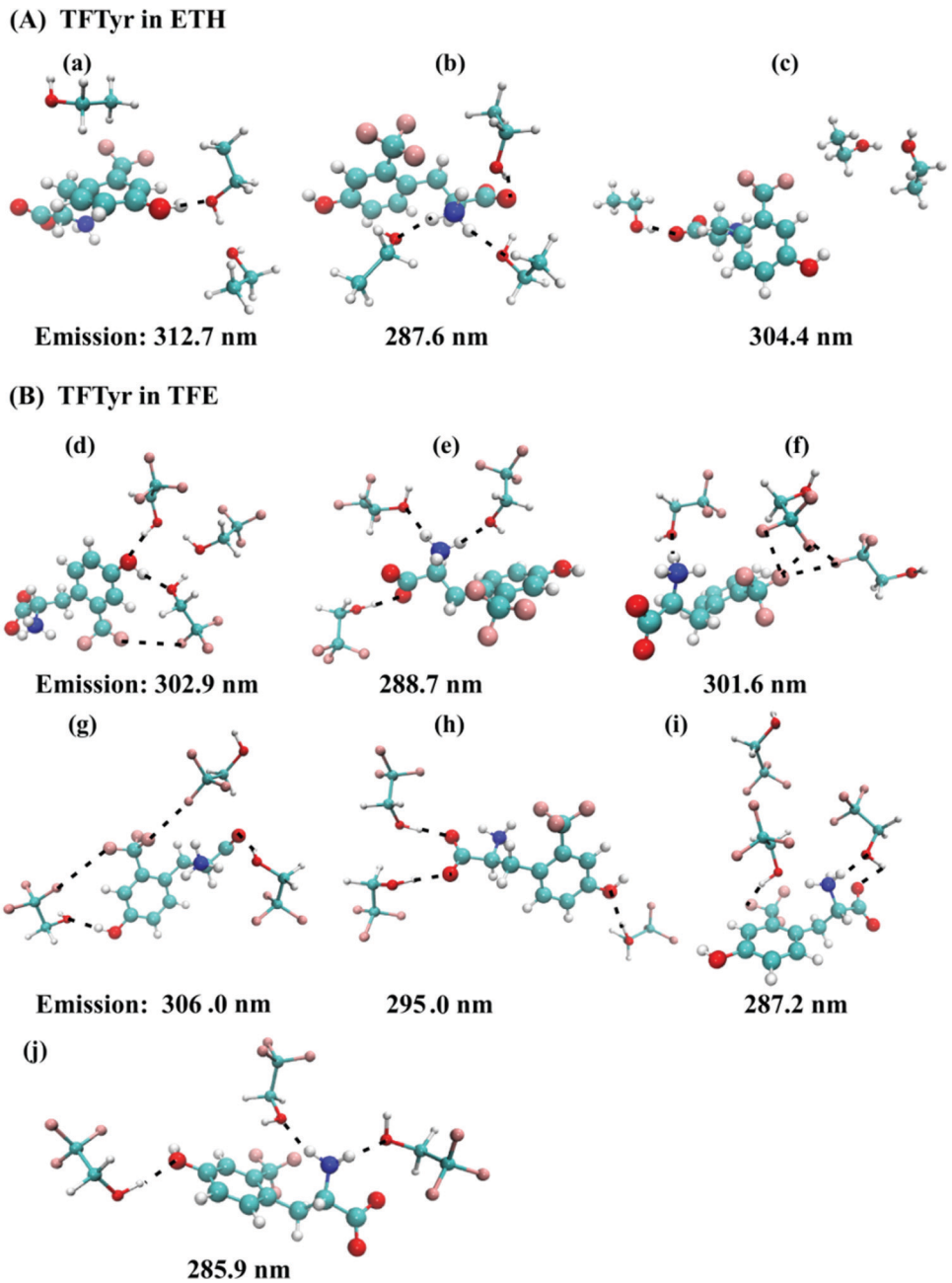

Fig. 6 The ground state optimized structures of TFTyr in ETH and TFE at different solvent binding sites. The calculated values of the peak maxima of the emission spectra are given below each corresponding structure.

different binding sites of TFTyr (OH, CF_3 and amino acid side chain containing COO^- and NH_3^+ groups), whose ground state structures are shown in Fig. S9 (ESI†) and Fig. 6. We have also compared the calculated emission maxima (Table 2) of different optimized structures of 1 : 3 clusters of TFTyr in ETH and TFE to substantiate the role of the $-CF_3$ group in TFTyr in its fluorescence properties. The calculated values of the emission maxima of all the structures of 1 : 1 clusters of TFTyr and TFE are in good agreement with the experimental values (Fig. S9, ESI†). In particular, the emission maximum of the structure (labeled a, Fig. S9 ESI,† emission value ~307 nm) with an O–H···O contact along with an F···F interaction is very close to its experimental value (308 nm). Similarly, the emission maxima of the structures (labeled e, f and g, Fig. S9, emission values 308, 309 and 307 nm, ESI†) having both O–H···O as well as F···F interactions are close to the experimental values. The emission maxima of the structures of 1 : 3 clusters of TFTyr and TFE having O–H···O, N–H···O as well as F···F interactions (structures d, f and g, Fig. 6, ~302–306 nm) are close to the experimental values. However, the emission maxima of the structures of 1 : 3 clusters of TFTyr-TFE (structures e, h, i, j, Fig. 6, emission value ~286 nm) which do not contain the F···F interaction are slightly less than the experimental value (308 nm). In contrast to the 1 : 3 cluster of TFE, the calculated value of the emission maximum of TFTyr in ETH is closer to the experimental data (312 nm); these clusters are predominantly hydrogen bonded *via* the chromophoric OH group of TFTyr (structures a and c of Fig. 6, emission values ~312 and 305 nm). Indeed, we have confirmed the presence of F···F interaction between TFTyr and TFE by performing an Atoms-in-Molecules (AIM) calculation, which shows the presence of a (3, −1) bond critical point at the F···F contacts[55] (Fig. S10, ESI†). Finally, we have calculated the emission maxima of TFTyr with ten TFE molecules using the ONIOM method[56] in which the CAM-B3LYP/6-31+G(d,p) level of theory was applied to the probe molecule while the solvent molecules were treated with RHF/3-21G(d). The optimized structure of the system is shown in Fig. S11 (ESI†), which clearly shows that TFE molecules are orientated with their terminal fluorines around the CF_3 along with several O–H···O as well as N–H···O contacts. The calculated value of the emission maximum of TFTyr was found at 302 nm, which is close to the experimental value. The calculated emission maxima of the different-sized clusters of TFTyr and TFE suggest that the role of the F···F, O–H···O and N–H···O interactions is significant in the probe's fluorescence behaviour.

The photophysical experiments, quantum chemical calculations as well as MD simulations suggest that the fluorescence behaviours of Tyr in different alcoholic solvents are determined mainly by the polarity of the medium, whereas, in the case of TFTyr, the different kinds of solute–solvent interactions control its fluorescence properties. The quantum chemical calculations along with the MD simulations suggest that the CF_3 group of TFTyr is responsible for the solvent-dependent differences in solvent organization around this noncanonical amino acid, which probably causes its solvent-dependent fluorescence behaviour in fluorinated-ETHs.

Conclusions

We have investigated the fluorescence behaviors of the noncanonical amino acid TFTyr in different alcoholic solvents, namely, ETH, MFE and TFE, and compared them with those of the natural amino acid derivative Tyr in the same solvents to understand the role of the noncanonical CF_3 moiety of the amino acid in the fluorescence properties. The excited state lifetime of Tyr decreases monotonically with the increase of fluorination of ETH, which clearly shows that the polarity of the medium controls the fluorescence properties of Tyr. In contrast, the excited state lifetime of TFTyr increases in the fluoroalcoholic solvents. The quantum chemical calculations and MD simulations suggest that the solvent orientation around the CF_3 group of TFTyr controls its fluorescence properties. The calculated emission maxima of different-sized clusters of TFTyr and TFE suggest that the role of F···F, O–H···O and N–H···O interactions is significant. This study suggests that solvent interactions with the fluorocarbon group of noncanonical amino acids are the cause of their diverse fluorescence behaviours, which implies their usefulness as solvent-sensitive environmental sensors in many biological processes.

Conflicts of interest

There are no conflicts to declare.

Acknowledgements

This work is supported partially by research grants provided by the Council of Scientific and Industrial Research (CSIR) [Grant No. 01(2803)/14/EMR-II] as well as the Department of Science and Technology (DST-SERB) [Grant No. EMR/2015/001605] India. T. N. and S. M. thank CSIR, institute, respectively, for their fellowships.

References

1 T. S. Young and P. G. Schultz, *J. Biol. Chem.*, 2010, **285**, 11039.
2 E. G. Worst, M. P. Exner, A. De Simone, M. Schenkelberger, V. Noireaux, N. Budisa and A. Ott, *J. Visualized Exp.*, 2016, 54273.
3 A. J. Link, M. L. Mock and D. A. Tirrell, *Curr. Opin. Biotechnol.*, 2003, **14**, 603.
4 N. Budisa, *Angew. Chem., Int. Ed.*, 2004, **43**, 6426.
5 L. Wang, J. Xie and P. G. Schultz, *Annu. Rev. Biophys. Biomol. Struct.*, 2006, **35**, 225.
6 C. C. Liu and P. G. Schultz, *Annu. Rev. Biochem.*, 2010, **79**, 413.
7 J. A. Johnson, Y. Y. Lu, J. A. Van Deventer and D. A. Tirrell, *Curr. Opin. Chem. Biol.*, 2010, **14**, 774.
8 D. A. Dougherty, *Curr. Opin. Chem. Biol.*, 2000, **4**, 645.
9 T. Hohsaka and M. Sisido, *Curr. Opin. Chem. Biol.*, 2002, **6**, 809.
10 M. Ibba and H. Hennecke, *FEBS Lett.*, 1995, **364**, 272.

11 J. T. Ngo and D. A. Tirrell, *Acc. Chem. Res.*, 2011, **44**, 677.
12 S. B. Sun, P. G. Schultz and C. H. Kim, *ChemBioChem*, 2014, **15**, 1721.
13 C. H. Kim, J. Y. Axup and P. G. Schultz, *Curr. Opin. Chem. Biol.*, 2013, **17**, 412.
14 M. Gomez-Nunez, K. J. Haro, T. Dao, D. Chau, A. Won, S. Escobar-Alvarez, V. Zakhaleva, T. Korontsvit, D. Y. Gin and D. A. Scheinberg, *PLoS One*, 2008, **3**, e3938.
15 N. Budisa, W. Wenger and B. Wiltschi, *Mol. BioSyst.*, 2010, **6**, 1630.
16 T. He, A. Gershenson, S. J. Eyles, Y.-J. Lee, W. R. Liu, J. Wang, J. Gao and M. F. Roberts, *J. Biol. Chem.*, 2015, **290**, 19334.
17 N. K. Mishra, A. K. Urick, S. W. J. Ember, E. Schönbrunn and W. C. Pomerantz, *ACS Chem. Biol.*, 2014, **9**, 2755.
18 N. C. Yoder and K. Kumar, *Chem. Soc. Rev.*, 2002, **31**, 335.
19 B. Bilgiçer, X. Xing and K. Kumar, *J. Am. Chem. Soc.*, 2001, **123**, 11815.
20 B. Bilgiçer and K. Kumar, *Tetrahedron*, 2002, **58**, 4105.
21 K.-H. Lee, H.-Y. Lee, M. M. Slutsky, J. T. Anderson and E. N. G. Marsh, *Biochemistry*, 2004, **43**, 16277.
22 B. C. Buer, B. J. Levin and E. N. G. Marsh, *J. Am. Chem. Soc.*, 2012, **134**, 13027.
23 B. C. Buer and E. N. G. Marsh, *Protein Sci.*, 2012, **21**, 453.
24 K. Muller, C. Faeh and F. Diederich, *Science*, 2007, **317**, 1881.
25 J. D. Dunitz, *ChemBioChem*, 2004, **5**, 614.
26 J. C. Biffinger, H. W. Kim and S. G. DiMagno, *ChemBioChem*, 2004, **5**, 622.
27 S. Mondal, S. Chaterjee, R. Halder, B. Jana and P. C. Singh, *J. Phys. Chem. B*, 2017, **121**, 7681.
28 S. Mondal, R. Halder, B. Biswas, B. Jana and P. C. Singh, *J. Chem. Phys.*, 2016, **144**, 184504.
29 O.-H. Kwon, T. H. Yoo, C. M. Othon, J. A. Van Deventer, D. A. Tirrell and A. H. Zewail, *Proc. Natl. Acad. Sci. U. S. A.*, 2010, **107**, 17101.
30 J. Xu, B. Chen, P. Callis, P. L. Muino, H. Rozeboom, J. Broos, D. Toptygin, L. Brand and J. R. Knutson, *J. Phys. Chem. B*, 2015, **119**, 4230.
31 S. S. Sarkar, J. B. Udgaonkar and G. Krishnamoorthy, *J. Phys. Chem. B*, 2011, **115**, 7479.
32 I. A. McDonald, P. L. Nyce, M. J. Jung and J. S. Sabol, *Tetrahedron Lett.*, 1991, **32**, 887.
33 B. Biswas, S. Mondal and P. C. Singh, *J. Phys. Chem. A*, 2017, **121**, 1250.
34 S. Mondal, B. Biswas, S. Sarkar and P. C. Singh, *J. Mol. Liq.*, 2017, **240**, 708.
35 M. J. Abraham, D. van der Spoel, E. Lindahl and B. Hess, and the GROMACS development team, 2016.
36 M. Lundborg and E. Lindahl, *J. Phys. Chem. B*, 2015, **119**, 810.
37 M. Fioroni, K. Burger, A. E. Mark and D. Roccatano, *J. Phys. Chem. B*, 2000, **104**, 12347.
38 J. T. Gerig, *J. Phys. Chem. B*, 2014, **118**, 1471.
39 S. Canzar, M. El-Kebir, R. Pool, K. Elbassioni, A. E. Mark, D. P. Geerke, L. Stougie and G. W. Klau, *J. Comput. Biol.*, 2013, **20**, 188.
40 C. I. Bayly, P. Cieplak, W. Cornell and P. A. Kollman, *J. Phys. Chem.*, 1993, **97**, 10269.
41 H. J. C. Berendsen, J. P. M. Postma, W. F. van Gunsteren, A. DiNola and J. R. Haak, *J. Chem. Phys.*, 1984, **81**, 3684.
42 M. Parrinello and A. Rahman, *J. Appl. Phys.*, 1981, **52**, 7182.
43 N. C. Yoder and K. Kumar, *Chem. Soc. Rev.*, 2002, **31**, 335.
44 F. Mohamadi, N. G. J. Richards, W. C. Guida, R. Liskamp, M. Lipton, C. Caufield, G. Chang, T. Hendrickson and W. C. Still, *J. Comput. Chem.*, 1990, **11**, 440.
45 K. Okuno, Y. Shigeta, R. Kishi, H. Miyasaka and M. Nakano, *J. Photochem. Photobiol., A*, 2012, **235**, 29.
46 T. Yanai, D. P. Tew and N. C. Handy, *Chem. Phys. Lett.*, 2004, **393**, 51.
47 A. V. Kulinich, N. A. Derevyanko, A. A. Ishchenko, N. B. Gusyak, I. M. Kobasa, P. P. Romańczyk and S. S. Kurek, *Dyes Pigm.*, 2019, **161**, 24.
48 S. Olsztynska-Janus, K. Szymborska, M. Komorowska and J. Lipinski, *J. Mol. Struct.*, 2009, **911**, 1.
49 C. K. Kim, B.-H. Park, H. W. Lee and C. K. Kim, *Org. Biomol. Chem.*, 2013, **11**, 1407.
50 A. V. Marenich, C. J. Cramer and D. G. Truhlar, *J. Phys. Chem. B*, 2009, **113**, 6378.
51 S. Miertuš, E. Scrocco and J. Tomasi, *Chem. Phys.*, 1981, **55**, 117.
52 J. Tomasi, B. Mennucci and R. Cammi, *Chem. Rev.*, 2005, **105**, 2999.
53 M. J. Frisch, G. W. Trucks, H. B. Schlegel, G. E. Scuseria, M. A. Robb, J. R. Cheeseman, G. Scalmani, V. Barone, G. A. Petersson, H. Nakatsuji, X. Li, M. Caricato, A. V. Marenich, J. Bloino, B. G. Janesko, R. Gomperts, B. Mennucci, H. P. Hratchian, J. V. Ortiz, A. F. Izmaylov, J. L. Sonnenberg, D. Williams-Young, F. Ding, F. Lipparini, F. Egidi, J. Goings, B. Peng, A. Petrone, T. Henderson, D. Ranasinghe, V. G. Zakrzewski, J. Gao, N. Rega, G. Zheng, W. Liang, M. Hada, M. Ehara, K. Toyota, R. Fukuda, J. Hasegawa, M. Ishida, T. Nakajima, Y. Honda, O. Kitao, H. Nakai, T. Vreven, K. Throssell, J. A. Montgomery Jr., J. E. Peralta, F. Ogliaro, M. J. Bearpark, J. J. Heyd, E. N. Brothers, K. N. Kudin, V. N. Staroverov, T. A. Keith, R. Kobayashi, J. Normand, K. Raghavachari, A. P. Rendell, J. C. Burant, S. S. Iyengar, J. Tomasi, M. Cossi, J. M. Millam, M. Klene, C. Adamo, R. Cammi, J. W. Ochterski, R. L. Martin, K. Morokuma, O. Farkas, J. B. Foresman and D. J. Fox, *Gaussian 09, Revision A.02*, Wallingford, CT, 2016.
54 R. J. Cave and E. W. Castner, Jr., *J. Phys. Chem. A*, 2002, **106**, 12117.
55 M. A. J. Márquez, M. A. B. Márquez, P. G. Cataldo and S. A. Brandán, *Open J. Synth. Theory Appl.*, 2015, **4**(1), 19.
56 L. W. Chung, W. M. C. Sameera, R. Ramozzi, A. J. Page, M. Hatanaka, G. P. Petrova, T. V. Harris, X. Li, Z. Ke, F. Liu, H.-B. Li, L. Ding and K. Morokuma, *Chem. Rev.*, 2015, **115**, 5678.

